Scattering Function of Oligo- and Polystyrenes in Dilute Solutions

Hitoshi Koyama, Takenao Yoshizaki, Yoshiyuki Einaga, Hisao Hayashi,† and Hiromi Yamakawa*

Department of Polymer Chemistry, Kyoto University, Kyoto 606, Japan

Received May 9, 1990; Revised Manuscript Received August 10, 1990

ABSTRACT: The scattering function $P_s(k)$ was measured for five samples of atactic oligo- and polystyrenes (a-PS), each with the fraction of racemic diads $f_r = 0.59$, in the range of weight-average molecular weight M_w from 1.48×10^3 to 4.0×10^4 in cyclohexane at 34.5 °C (Θ) for $k \lesssim 0.5$ Å^{-1} by the use of a point-focusing small-angle X-ray scattering (SAXS) camera, where k is the magnitude of the scattering vector. The measurements were also carried out for a sample with $M_w = 1.01 \times 10^4$ in *trans*-decalin at 21.2 °C (Θ) in order to examine the effect of the environment. For $k \lesssim 0.25$ Å^{-1}, all the experimental data may well be explained by the helical wormlike (HW) chain theory with the model parameters previously determined for the same a-PS chain, assuming the cylinder model for the electron distribution around the HW chain contour. The diameter of the cylinder determined from the data analysis increases with increasing M_w for $M_w \lesssim 1.0 \times 10^4$, indicating that the proximity of two repeat units in the same chain enlarges apparently the effective chain thickness. For large k, the experimental results of P_s somewhat differ in the two solvents, exhibiting the dependence on the environment. In this connection, a comparison of the present SAXS data with the small-angle neutron scattering data obtained by Huber et al. is also made, and it is shown that the effective diameter determined from the former is larger than that from the latter, as was expected.

Introduction

In a series of experimental studies of dilute-solution properties of atactic oligo- and polystyrenes (a-PS) with the fraction of racemic diads $f_r = 0.59$ (in the Θ state), we have already measured the mean-square optical anisotropy $\langle \Gamma^2 \rangle$,[1] intrinsic viscosity $[\eta]$,[2] and mean-square radius of gyration $\langle S^2 \rangle$[3] over a wide range of molecular weight, including the oligomers, and shown that the results may well be explained consistently by the helical wormlike (HW) chain theory.[4,5] We have also shown explicitly the difference between the a-PS and atactic poly(methyl methacrylate) with $f_r = 0.79$ in local chain conformation, giving a picture of instantaneous contours of HW Monte Carlo chains generated with the model parameters determined for them.[7] Recall here that the HW model parameters are the constant curvature κ_0 and torsion τ_0 of the characteristic regular helix taken at the minimum of energy, the stiffness parameter λ^{-1} as defined as the bending force constant divided by $k_B T/2$, with k_B the Boltzmann constant and T the absolute temperature, and the shift factor M_L as defined as the molecular weight per unit contour length. In the present paper of this series, we proceed to further investigate the scattering function P_s for the a-PS by small-angle X-ray scattering (SAXS) measurements to examine whether the experimental results may be explained by the HW theory with the model parameters previously determined.[3]

Now, in almost all of SAXS measurements carried out so far for dilute polymer solutions[8] except for a few recent ones,[9,10] P_s was determined by desmearing scattering intensities measured by the use of a Kratky camera.[11] However, this procedure may be considered to be inadequate for a determination of P_s in the range of large k, with k the magnitude of the scattering vector, since the excess scattering intensity there by solute polymers becomes very weak and it may possibly cause appreciable errors also because of the geometrical limitation of the camera itself. Thus, in the present study, in order to remove this difficulty, we used a point-focusing camera that required no desmearing.

† Present address: Department of Materials Chemistry, Faculty of Science and Technology, Ryukoku University, Seta, Otsu 520-21, Japan.

An analysis of experimental data for the actually observed scattering function P_s is made by the use of the HW theory developed in the preceding paper,[12] which takes account of the effect of the distribution of electrons around the chain contour, i.e., the chain thickness. In order to obtain our profound understanding of the effects of the environment and of the local spatial distribution of scatterers, we carried out measurements in two Θ solvents and also make a comparison of the present SAXS results with those from small-angle neutron scattering (SANS) measurements.

Experimental Section

Materials. The a-PS samples used in this work are fractions separated from standard samples A-1000, A-2500, A-5000, F-1, and F-4 supplied by Tosoh Co., Ltd., by preparative gel permeation chromatography (GPC) or fractional precipitation. All the samples are the same ones as used in the previous study of $\langle S^2 \rangle$.[3] They are sufficiently narrow in moelcular weight distribution and have a fixed stereochemical composition of $f_r = 0.59$ independent of the molecular weight. The values of the weight-average molecular weight M_w determined from light scattering measurements are listed in Table I along with the ratios of M_w to the number-average molecular weight M_n determined by analytical GPC. Also listed in Table I are the root-mean-square radii of gyration $\langle S^2 \rangle^{1/2}$ from SAXS measurements.

The solvent cyclohexane used for the SAXS measurements was purified according to a standard procedure. Reagent grade *trans*-decalin (Wako, 97% purity) was used as another solvent after distillation under reduced pressure. Its purity was examined by gas chromatography, and no peak corresponding to the cis component could be detected. Test solutions were prepared gravimetrically, and their polymer mass concentrations c in g/cm^3 were calculated from their weight fractions with the solution density data obtained, as described previously.[1,2]

Small-Angle X-ray Scattering. All SAXS measurements were carried out by the use of a point-focusing SAXS camera of overall length of 6 m in the High-Intensity X-ray Laboratory of Kyoto University. Although a rather detailed specification of this camera has already been given elsewhere,[13] we here reproduce it briefly for convenience.

The X-ray source is a rotating-anode generator (RU-1000C3, Rigaku Corp., Japan), the maximum power being 3.5 kW for a copper anode. A double-mirror focusing system of the Franks type is adopted as a collimator, it consisting of a pair of crossed-

0024-9297/91/2224-0932$02.50/0

Table I
Values of M_w, M_w/M_n, and $\langle S^2\rangle^{1/2}$ for Atactic Polystyrenes with $f_r = 0.59$ in Cyclohexane at 34.5 °C

sample	M_w	M_w/M_n	$\langle S^2\rangle^{1/2}$, Å
A1000-b	1480	1.02	7.99
A2500-a	2270	1.05	11.2
A5000-3	5380	1.03	19.0
F1-2	10100	1.03	27.3
F4	40000	1.02	56.6

plane total-reflection mirrors, each of 40 cm in length. The mirrors are gold coated. [The beam size is 2 (vertical) × 1.5 mm (horizontal) in the case of quartz mirrors.] The detector is a two-dimensional position-sensitive proportional counter with multiwire delay lines manufactured by Rigaku Corp., Japan, and has an active area of 128 × 128 mm with a spatial resolution of 0.5 × 1.0 mm. The distance from the sample to the detector can be varied from ca. 0.5 to 3 m at 0.5-m intervals to cover scattering angles from 0.001 to 0.18 rad. The air in the path of the incident and scattered radiations and also in the sample and detector chambers is evacuated to prevent scattering from it.

In the present study, the Cu Kα line of wavelength $\lambda_0 = 1.54$ Å was used as the incident beam by eliminating other lines with a Ni foil of 10-μm thickness. A sample solution is filled in a sample cell newly designed for the present study. It is a brass block having a hollow space with thin detachable mica windows, its optical path being about 1.8 mm in length. It has an inlet and an outlet, both of airtight structure, to facilitate exchange of sample solutions or solvents for successive measurements. The cell is fixed to a holder in the sample chamber. For the present study, it was located at the position of 640 ± 3 mm from the detector plane, so that intensity measurements could be carried out in the range of the magnitude k of the scattering vector up to ca. 0.5 Å^{-1}. Its temperature was kept constant at 34.5 ± 0.1 °C for cyclohexane solutions and at 21.2 ± 0.1 °C for *trans*-decalin solutions.

The two-dimensional data for a solution of concentration c were first corrected for the detector sensitivity and then averaged over polar angles in the detector plane to obtain the scattering intensity $I_{obs}(k,c)$ as a function of k

$$k = (4\pi/\lambda_0)\sin(\theta/2) \tag{1}$$

with θ the scattering angle. From the observed intensity I_{obs}, we evaluate the reduced intensity $I_R(k,c)$, defined by

$$I_R(k,c) = \frac{I_{obs}(k,c)}{AI_0} \tag{2}$$

where A is the transmittance of a given sample solution and I_0 is the intensity of the incident beam monitored by the scattering intensity from a high-density polyethylene film placed in front of the detector. The excess reduced scattering intensity $\Delta I_R(k,c)$ is evaluated as the reduced scattering intensity from the solution $I_{R,soln}(k,c)$ minus that from the solvent $I_{R,solv}(k)$

$$\Delta I_R(k,c) = I_{R,soln}(k,c) - I_{R,solv}(k) \tag{3}$$

Results

For convenience, we begin by giving the basic equation for the excess reduced scattering intensity $\Delta I_R(k,c)$ defined by eq 3 necessary for an experimental determination of the scattering function $P_s(k)$. It reads

$$\frac{Kc}{\Delta I_R(k,c)} = \frac{1}{M_w P_s(k)} + 2A_2Q(k)c + \mathcal{O}(c^2) \tag{4}$$

where K is the optical constant, A_2 is the second virial coefficient, and Q represents the intermolecular interferences.[14] Note that P_s and Q become unity at $k = 0$. In the case of SAXS, K is given by

$$K = N_A I_e V \varphi_A \Delta z_e^2 \tag{5}$$

where N_A is Avogadro's number, I_e is the Thomson factor (7.90×10^{-26} cm^2), V is the scattering volume, φ_A is the apparatus constant, and Δz_e is the mole number of effective electrons per unit gram of the solute polymer[15] and is given by

$$\Delta z_e = (n_2/M_0) - (v_2\rho_0 n_1/M_s) \tag{6}$$

In eq 6, n_2 and M_0 are the number of electrons and the molecular weight per repeat unit of the polymer, respectively, v_2 is the partial specific volume of the polymer, ρ_0 is the density of the solvent, and n_1 and M_s are the number of electrons and the molecular weight of the solvent molecule, respectively. The values 0.7653 and 0.8686 g/cm^3 were used for ρ_0 of cyclohexane at 34.5 °C (Θ) and *trans*-decalin at 21.2 °C (Θ),[16] respectively, and the values of v_2 were determined from density measurements.

Now we consider the ratio $\Delta I_R(k,c)/\Delta I_R(0,c)$, i.e., an apparent scattering function at finite concentrations. It may be written, from eq 4, as

$$\frac{\Delta I_R(k,c)}{\Delta I_R(0,c)} = P_s(k) + 2A_2M_wP_s(k)[1 - P_s(k)\,Q(k)]c + \mathcal{O}(c^2) \tag{7}$$

According to this equation, P_s may be determined by extrapolation of the ratio to $c = 0$. For this purpose, we must first determine $\Delta I_R(0,c)$, for instance, by the square root plot[16] of $c/\Delta I_R$. With the data for the two samples A1000-b and A2500-a (of the lowest M_w), it was found that the plot of $(c/\Delta I_R)^{1/2}$ against k^2 followed a straight line in the range of small k for each sample in cyclohexane at 34.5 °C, so that the intercept $[c/\Delta I_R(0,c)]^{1/2}$ at a given c could be unambiguously determined.

However, for the other samples with higher molecular weights listed in Table I, such a plot no longer followed a straight line, and we could not determine $\Delta I_R(0,c)$. For these samples, therefore, we consider, instead of the ratio in eq 7, the ratio $\Delta I_R(k,c)/KM_wc$, which may be written, from eq 4, as

$$\frac{\Delta I_R(k,c)}{KM_wc} = P_s(k) - 2A_2M_w[P_s(k)]^2Q(k)c + \mathcal{O}(c^2) \tag{8}$$

Thus P_s may also be determined by extrapolation of this ratio to $c = 0$ if the value of K is known. In general, the value of K may be calculated from eq 5 if the values of Δz_e and the apparatus constant φ_A' redefined by $\varphi_A' = N_A I_e V \varphi_A$ are known; i.e.

$$K = \varphi_A' \Delta z_e^2 \tag{9}$$

Note that φ_A' is a constant independent of polymer and solvent, so that its value, once determined, may be used for any other polymer–solvent system.

The value of φ_A' may be calculated from the relation

$$\varphi_A' = [\Delta I_R(0,c)/c]_{c=0}/\Delta z_e M_w \tag{10}$$

with the known values of Δz_e and M_w for a given system. Here, the values of $[\Delta I_R(0,c)/c]_{c=0}$ could be determined for samples A1000-b and A2500-a in cyclohexane at 34.5 °C as follows. As mentioned above, the intercept $[c/\Delta I_R(0,c)]^{1/2}$ could be determined for each of them. Similarly, in the range of small k, the plot of $[c/\Delta I_R(k,c)]^{1/2}$ against c was fitted by a straight line and could be extrapolated to $c = 0$ to evaluate $[c/\Delta I_R(k,c)]_{c=0}^{1/2}$ at a given (small) k. The values of $[c/\Delta I_R(0,c)]^{1/2}$ and $[c/\Delta I_R(k,c)]_{c=0}^{1/2}$ thus obtained are plotted against c and k^2, respectively, in Figure 1 for the above two samples. The two kinds of plots are fitted by straight lines and can be extrapolated to determine the common intercept $[c/\Delta I_R(0,c)]_{c=0}^{1/2}$. The values of φ_A' thus obtained for samples A1000-b and A2500-a are 1.54×10^4 and 1.60 ×

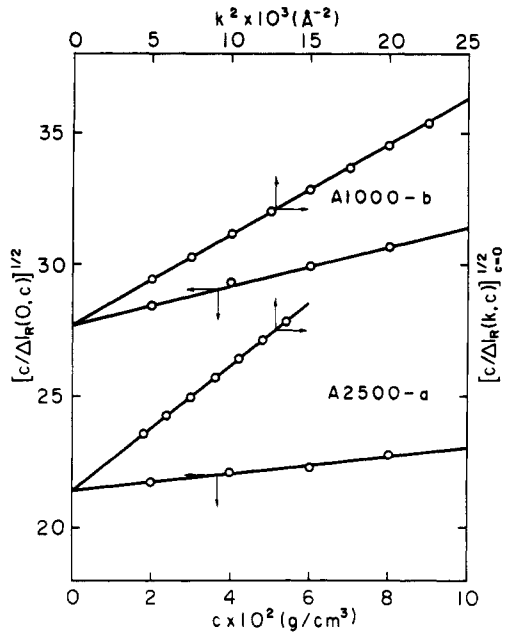

Figure 1. Plots of $[c/\Delta I_R(0,c)]^{1/2}$ and $[c/\Delta I_R(k,c)]_{c=0}^{1/2}$ against c and k^2, respectively, for samples A1000-b and A2500-a in cyclohexane at 34.5 °C.

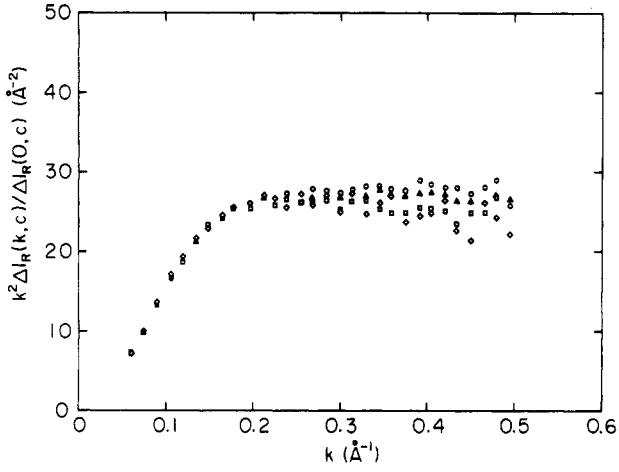

Figure 2. Plots of $k^2\Delta I_R(k,c)/\Delta I_R(0,c)$ against k for sample A2500-a in cyclohexane at 34.5 °C: (○) c = 0.0806 g/cm³; (△) c = 0.0600 g/cm³; (□) c = 0.0397 g/cm³; (◇) c = 0.0200 g/cm³.

10^4 cm³/g, respectively. In what follows, we use the mean value 1.57×10^4 cm³/g for φ_A'.

The two ratios in eqs 7 and 8 take the same value $P_s(k)$ at a given k in the limit of $c = 0$ but, in general, different values at finite concentrations. Figures 2 and 3 show plots of $k^2\Delta I_R(k,c)/\Delta I_R(0,c)$ and $k^2\Delta I_R(k,c)/KM_wc$ against k, respectively, for sample A2500-a in cyclohexane at 34.5 °C. In both figures, the circles, triangles, squares, and diamonds represent the values at c = 0.0806, 0.0600, 0.0397, and 0.0200 g/cm³, respectively. The two ratios differ from each other in the dependence on c but almost coincide with each other at the lowest concentration. Thus we adopt the values of $\Delta I_R(k,c)/KM_wc$ at the lowest concentration as those of the scattering function $P_s(k)$ for the single polymer chain (at infinite dilution).

In order to display the data, it is convenient to consider the scattering function $\tilde{F}_s(k)$ defined by

$$\tilde{F}_s(k) = M_w k^2 P_s(k) \tag{11}$$

instead of $P_s(k)$ itself. It is related to the scattering function $F_s(k)$ defined in the preceding paper[12] by the

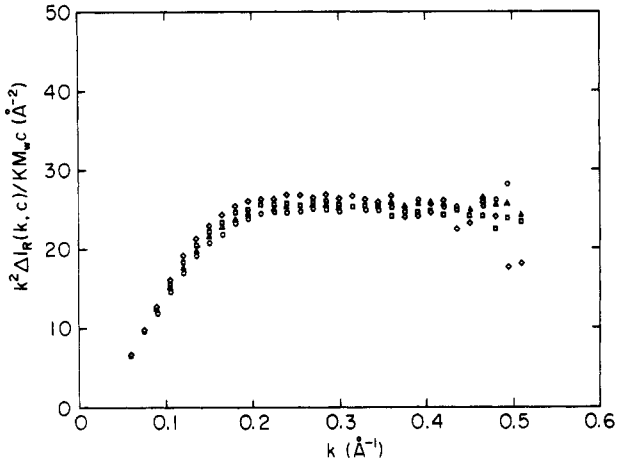

Figure 3. Plots of $k^2\Delta I_R(k,c)/KM_wc$ against k for sample A2500-a in cyclohexane at 34.5 °C; see legend for Figure 2.

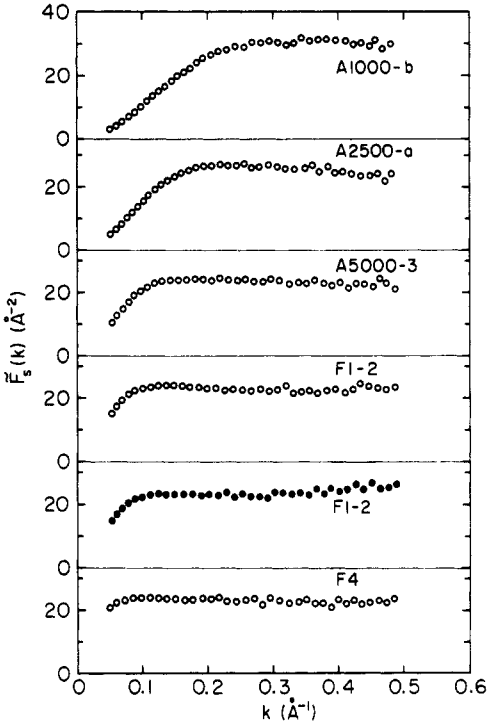

Figure 4. Plots of $\tilde{F}_s(k)$ against k for all the samples in cyclohexane at 34.5 °C and for sample F1-2 in *trans*-decalin at 21.2 °C: (○) in cyclohexane; (●) in *trans*-decalin.

equation

$$\tilde{F}_s(k) = M_L F_s(k) \tag{12}$$

Figure 4 shows plots of $\tilde{F}_s(k)$ against k for all the samples in cyclohexane at 34.5 °C (Θ) along with those for sample F1-2 in *trans*-decalin at 21.2 °C (Θ). We note that for the plot for F1-2 in *trans*-decalin, we have used the value of K calculated from eq 9 with the values of φ_A' determined above and Δz_e for this polymer–solvent system.

Discussion

Scattering Function. As shown in Figure 4, the data for the scattering function P_s or $\tilde{F}_s$ in the range of $k \lesssim 0.06$ Å^{-1} could not be obtained under the present setting condition of the sample-to-detector distance of the SAXS camera mentioned in the Experimental Section. Thus we use the previous data[3] for $\tilde{F}_s$ obtained in the range of small k by a Kratky U-slit camera and join them to the present data. However, the present data are seen to scatter rather

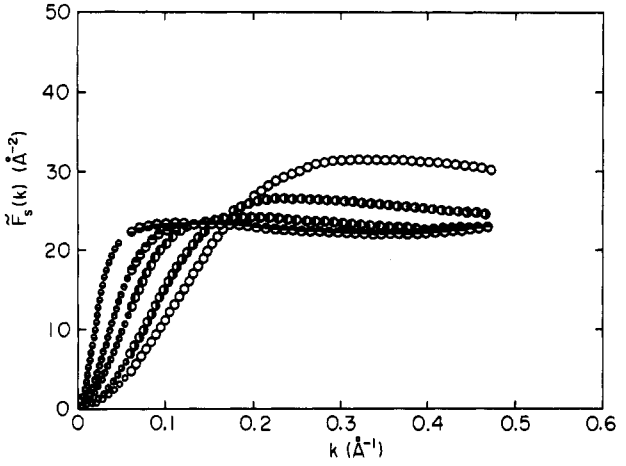

Figure 5. Plots of $\tilde{F}_s(k)$ against k for all the samples in cyclohexane at 34.5 °C: (○) A1000-b; (◑) A2500-a; (◐) A5000-3; (◓) F1-2; (◒) F4. The large and small circles represent the present and previous[3] data, respectively.

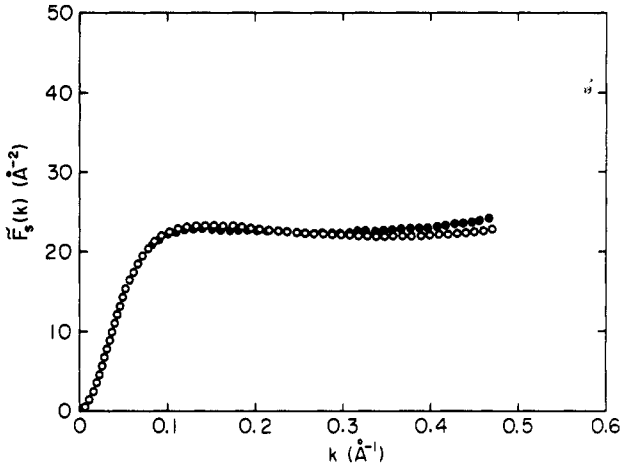

Figure 6. Plots of $\tilde{F}_s(k)$ against k for sample F1-2: (○) in cyclohexane at 34.5 °C; (●) in *trans*-decalin at 21.2 °C.

appreciably, and therefore we smooth them by assuming its most probable value as the "observed" value of $\tilde{F}_s$ at a given k.

Figure 5 shows plots of the data for $\tilde{F}_s(k)$ thus obtained against k for the a-PS samples in cyclohexane at 34.5 °C. The unfilled, right-half filled, left-half filled, top-half filled, and bottom-half filled circles represent the values for samples A1000-b, A2500-a, A5000-3, F1-2, and F4, respectively, the large and small circles representing the present and previous data, respectively. It is seen that the previous data are smoothly connected to the present data. This confirms the appropriateness and accuracy of our procedure of extrapolation to $c = 0$ described in the preceding section. The value of $\tilde{F}_s$ at fixed $k \lesssim 0.15$ Å^{-1} increases with increasing M_w, and the value of k at which $\tilde{F}_s$ exhibits a shoulder becomes small as M_w is increased. On the other hand, the value of $\tilde{F}_s$ at fixed $k \gtrsim 0.15$ Å^{-1} decreases with increasing M_w and becomes independent of M_w for $M_w \gtrsim 10^4$. This dependence of $\tilde{F}_s$ on M_w in the range of large k may not be predicted by any existing theory and will be discussed in the next subsection.

Next we examine the effect of the environment (solvent) on $\tilde{F}_s$. Figure 6 shows plots of $\tilde{F}_s(k)$ against k for sample F1-2 in cyclohexane at 34.5 °C and in *trans*-decalin at 21.2 °C. The values of $\tilde{F}_s$ for the two polymer–solvent systems agree for $k \lesssim 0.3$ Å^{-1} but somewhat separate from each other for larger k. Now recall that for large M_w, the a-PS chain has almost the same value of $\langle S^2 \rangle / M_w$ in the two Θ solvents[16] (which is consistent with the present results for F_s for small k), indicating that its local conformations in the two solvents do not appreciably differ. Therefore the difference between the two polymer–solvent systems in $\tilde{F}_s$ in the range of large k may be regarded as arising from the difference in the effective local electron density or the effective chain thickness.

Comparison with the HW Theory. Now we make a comparison of the experimental data for $\tilde{F}_s$ with the HW theory developed in the preceding paper,[12] where the effect of chain thickness has been taken into account by considering the two simple models for the electron distribution around the HW chain contour, i.e., the cylinder model and the touched-spheroid model. It has been shown that the theoretical values of P_s for the two models differ only in the range of large k for which the detailed structure of the local electron distribution has a significant influence on P_s. Thus we consider here only the cylinder model, for simplicity.

The scattering function $P_s(k;L)$ for the HW chain of total contour length L is given by eq 25 with eqs 36–41 of ref 12 and may be rewritten in the form

$$P_s(k;L) = 2L^{-2}\int_0^L (L-t)I(\mathbf{k};t)\{[F_0(kd)]^2 + g_2^{00}(t)[F_1(kd)]^2\}\,dt \quad (13)$$

where $I(\mathbf{k};t)$ is the characteristic function, i.e., the Fourier transform of the distribution function $G(\mathbf{R};t)$ of the end-to-end vector distance $\mathbf{R}$ for the HW chain of contour length t, F_n ($n = 0, 1$) are the functions of kd, with d the cylinder diameter (representing the form of the electron distribution) given by eqs 40 and 41 of ref 12, and g_2^{00} is the angular correlation function[17] given by eq 38 of ref 12. We note that the functions I and g_2^{00} depend on the HW model parameters and that $F_0(0) = 1$ and $F_1(0) = 0$, so that when $d = 0$, eq 13 gives the exact expression for P_s for the HW chain contour itself. For the calculation of the HW theoretical values for the a-PS chain with $f_r = 0.59$, we have used the model parameters[3] determined from an analysis of experimental data for $\langle \Gamma^2 \rangle$ and $\langle S^2 \rangle$: $\lambda^{-1}\kappa_0 = 3.0$, $\lambda^{-1}\tau_0 = 6.0$, $\lambda^{-1} = 22.5$ Å, and $M_L = 36.7$ Å^{-1}. The diameter d as an adjustable parameter has been determined from a best fit of the theoretical values to the data. Then recall that evaluation of the characteristic function I and the integral in eq 13 must be carried out numerically. All numerical work has been done by the use of a FACOM M-780 digital computer in this university.

Figure 7 shows plots of $\tilde{F}_s(k)$ against k for all the a-PS samples in cyclohexane at 34.5 °C. The solid curves represent the best-fit HW theoretical values. The values of d thus determined by the curve fitting are 6.8, 9.5, 12.2, 13.7, and 13.9 Å for samples A1000-b, A2500-a, A5000-3, F1-2, and F4, respectively. For all the samples, the agreement between the experimental and theoretical values is rather good in the range of $k \lesssim 0.25$ Å^{-1} but becomes poor for larger k, indicating that the details of electron distribution must there be taken into account.

In order to illustrate the dependence of d on M_w, its values are plotted against log M_w in Figure 8. The horizontal line segment indicates the value 9.4 Å of d that has been used in the previous study[3] to evaluate the squared radius of gyration S_c^2 of the cross section of the chain. It is seen that the present d increases monotonically with increasing M_w and becomes independent of M_w for $M_w \gtrsim 10^4$, this dependence (or independence) corresponding to that of $\tilde{F}_s$ at large k mentioned in the preceding subsection. This result may be understood as follows. As the chain length is increased, it becomes, to some extent,

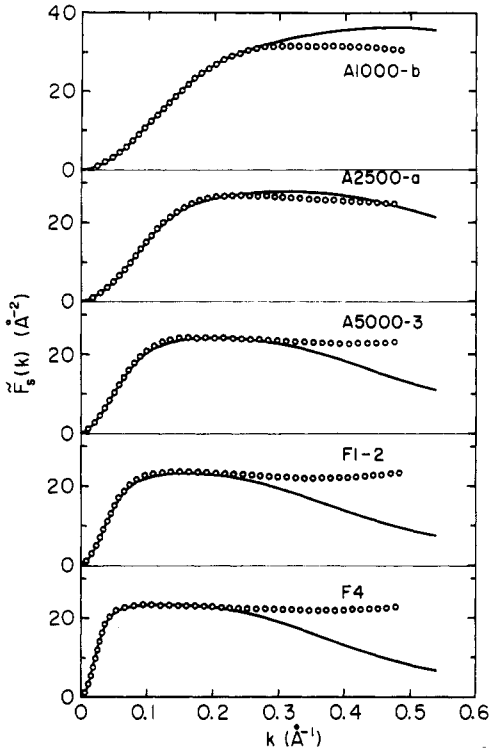

Figure 7. Comparison of the observed values of $\tilde{F}_s$ with the HW theoretical ones: (○) data in cyclohexane at 34.5 °C; solid curves, best-fit theoretical values calculated from eq 14.

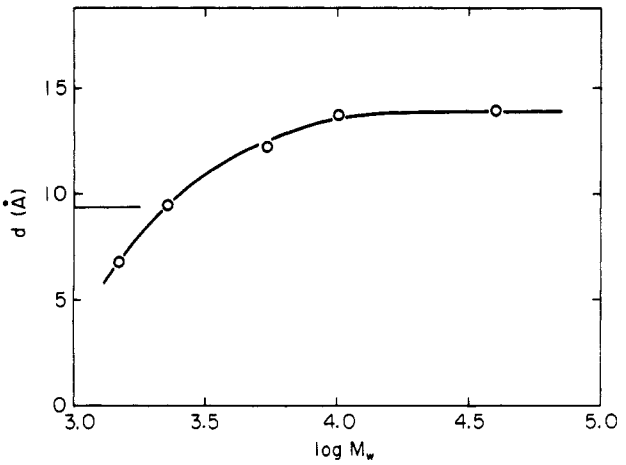

Figure 8. Dependence on M_w of d determined from the curve fitting. The horizontal line segment indicates the value of d used in the previous work.[3]

easier for two repeat units in the same chain to come close to each other, leading to the enlargement of the effective chain thickness. The situation is similar to the effect of the environment discussed above. At any rate, however, the present values of d may be regarded as consistent with the previous one.[3]

Effects of the Distribution of Scatterers. In this subsection, we make a comparison of the present SAXS data with the SANS data obtained by Huber et al.[18] for a-PS to examine the effect of the distribution of scatterers. Figure 9 shows plots of $\tilde{F}_s(k)$ against k. The unfilled circles represent the present SAXS data for sample F1-2 in cyclohexane at 34.5 °C, and the filled circles the SANS data for a Tosoh standard a-PS sample with M_w = 1.07 × 10^4 in cyclohexane-d_{12} at c = 0.0209 g/cm^3 and at 35 °C.[18] (The two samples come from the same source and may therefore be considered to have the same value of f_r.) It is seen that there is good agreement between the SAXS and SANS data for small k, while they differ appreciably for large k.

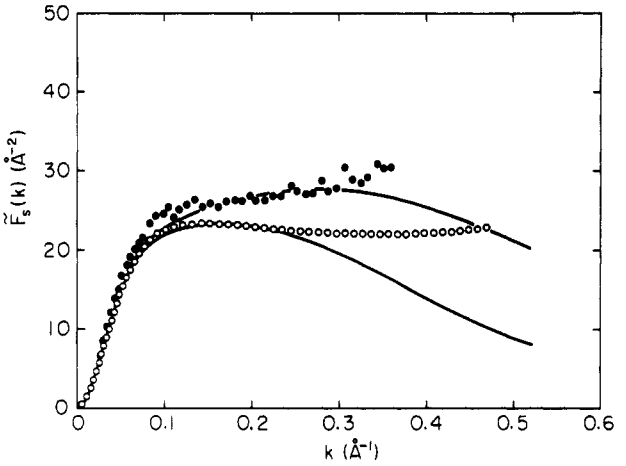

Figure 9. Comparison between SAXS and SANS data: (○) present SAXS data for sample F1-2 in cyclohexane at 34.5 °C; (●) SANS data for an a-PS sample with M_w = 1.07 × 10^4 in cyclohexane-d_{12} at c = 0.0209 g/cm^3 and at 35 °C by Huber et al.;[18] solid curves, best-fit theoretical values calculated from eq 14.

The solid curves in the figure represent the best-fit HW theoretical values. The value of d determined from the SANS data is 9.9 Å, which is smaller than the value 13.7 Å from the SAXS data. This disagreement may be regarded as arising from the fact that the distribution of electrons as the scatterers around the chain contour in SAXS is broader than that of hydrogen atoms as the scatterers in SANS if the local conformations of these a-PS chains do not differ. This is consistent with the previous finding[3] that the apparent mean-square radius of gyration $\langle S^2 \rangle_s$ from SAXS is appreciably larger than that from SANS in the oligomer region for the a-PS, which has not explicitly been mentioned (see Figure 8 of ref 3). (It has been shown by Huber et al.[19] that, although the Θ temperature for a-PS in cyclohexane-d_{12} is 38 °C and is somewhat higher than 35 °C, this difference in temperature has no influence on $\langle S^2 \rangle$.) Thus the present SAXS data are consistent with the SANS data of Huber et al.

Conclusion

The scattering functions P_s for the a-PS chains of various molecular weights, including the oligomers, each with the fraction of racemic diads f_r = 0.59, have been determined accurately in the Θ state by using the point-focusing SAXS camera in the High-Intensity X-ray Laboratory of Kyoto University. From a comparison of the experimental results with the HW theoretical values, it has been shown that the theory may provide satisfactory understanding of the observed scattering profiles in the range of $k \lesssim 0.25$ Å^{-1}. The value of 4 Å of this upper bound reciprocal just corresponds to several bond lengths, indicating that the present simple model for the distribution of electrons on the basis of the HW chain may be valid only on such HW length scales. For larger k, the details of the local distribution of scatterers as well as the local chain conformation have significant effects on P_s, as seen from a comparison between the SAXS and SANS data, and then the present theory breaks down. However, it seems difficult and even insignificant to analyze the data by considering the detailed distribution of scatterers on the basis of, for instance, the rotational isomeric state model.

Acknowledgment. This research was supported in part by a Grant-in-Aid (01430018) from the Ministry of

Education, Science, and Culture, Japan.

References and Notes

(1) Konishi, T.; Yoshizaki, T.; Shimada, J.; Yamakawa, H. *Macromolecules* **1989**, *22*, 1921.
(2) Einaga, Y.; Koyama, H.; Konishi, T.; Yamakawa, H. *Macromolecules* **1989**, *22*, 3419.
(3) Konishi, T.; Yoshizaki, T.; Saito, T.; Einaga, Y.; Yamakawa, H. *Macromolecules* **1990**, *23*, 290.
(4) Yamakawa, H.; Fujii, M. *J. Chem. Phys.* **1976**, *64*, 5222.
(5) Yamakawa, H.; Fujii, M.; Shimada, J. *J. Chem. Phys.* **1979**, *71*, 1611.
(6) Yoshizaki, T.; Nitta, I.; Yamakawa, H. *Macromolecules* **1988**, *21*, 165.
(7) Tamai, Y.; Konishi, T.; Einaga, Y.; Fujii, M.; Yamakawa, H. *Macromolecules* **1990**, *23*, 4067.
(8) Kirste, R. G.; Oberthür, R. C. In *Small Angle X-ray Scattering*; Glatter, O., Kratky, O., Eds.; Academic Press: New York, 1982; p 387.
(9) Hayashi, H.; Flory, P. J.; Wignall, G. D. *Macromolecules* **1983**, *16*, 1328.
(10) Muroga, Y.; Tagawa, H.; Hiragi, Y.; Ueki, T.; Kataoka, M.; Izumi, Y.; Amemiya, Y. *Macromolecules* **1988**, *21*, 2756.
(11) Glatter, O. In *Small Angle X-ray Scattering*; Glatter, O., Kratky, O., Eds.; Academic Press: New York, 1982; p 119.
(12) Nagasaka, K.; Yoshizaki, T.; Shimada, J.; Yamakawa, H. *Macromolecules*, preceding paper in this issue.
(13) Hayashi, H.; Hamada, F.; Suehiro, S.; Masaki, N.; Ogawa, T.; Miyaji, H. *J. Appl. Crystallogr.* **1988**, *21*, 330.
(14) Yamakawa, H. *Modern Theory of Polymer Solutions*; Harper & Row: New York, 1971; p 211.
(15) The statement concerning Δz_e in ref 3 is wrong; "sample solution" should be replaced by "solute polymer".
(16) Berry, G. C. *J. Chem. Phys.* **1966**, *44*, 4550.
(17) Yamakawa, H.; Shimada, J. *J. Chem. Phys.* **1979**, *70*, 609.
(18) Huber, K.; Burchard, W.; Bantle, S. *Polymer* **1987**, *28*, 863.
(19) Huber, K.; Bantle, S.; Lutz, P.; Burchard, W. *Macromolecules* **1985**, *18*, 1461.

Registry No. a-PS, 9003-53-6.